Physics and Chemistry of Minerals (2020) 47:28
https://doi.org/10.1007/s00269-020-01098-3

ORIGINAL PAPER

Effects of alkali and alkaline-earth cations on the high-pressure sound velocities of aluminosilicate glasses

Koji Aoki[1] · Tatsuya Sakamaki[2] · Tomonori Ohashi[2] · Osamu Ikeda[2] · Akio Suzuki[2]

Received: 20 December 2019 / Accepted: 19 May 2020 / Published online: 26 May 2020

Abstract

The sound velocities (compressional wave velocity [V_P] and shear wave velocity [V_S]) of four types of aluminosilicate glasses ($Mg_3Al_2Si_6O_{18}$ (MAS), $Ca_3Al_2Si_6O_{18}$ (CAS), $Na_3AlSi_3O_9$ (NAS), and $K_3AlSi_3O_9$ (KAS)) are measured using the ultrasonic technique at high pressures of up to 7.8 GPa. The V_P and V_S of MAS glass decrease up to a pressure of 2 GPa and subsequently increase with increasing pressure. The pressure dependence of the CAS glass velocities changes; V_P remains almost constant when $P \leq 2$ GPa and subsequently increases above 2 GPa. The minimum V_S can be observed at approximately 2 GPa, which is similar to that in the case of the MAS glass. The sound velocities of the NAS and KAS glasses monotonically increase with pressure. The increments in the V_P and V_S of the KAS glass show less sensitivity when compared with that observed in the case of the NAS glass within the pressure range of our experiments. The differences in the properties of the modifying cations in the glasses, such as size ($^{[5]}Mg^{2+} < {}^{[\sim 6-7]}Ca^{2+} \approx {}^{[\sim 6-7]}Na^{+} < {}^{[\sim 9-11]}K^{+}$) and field strength (ratio of the charge to the square radius), can be considered responsible for each sound velocity trend. The effects of the cation field strength on the structure and elasticity of the aluminosilicate glasses could govern the pressure-induced change in sound velocities. The results indicate that the type and amount of cation control the elastic behavior of silicate glass under high pressure.

Keywords Aluminosilicate glass · Network-modifying cation · Sound velocity · High pressure

Introduction

The nature of magma under high pressure is considerably related to the magmatic processes occurring in the Earth's interior. SiO_2 is the main component of magma, and its concentration significantly controls the magma mobility and eruption style. For example, magma becomes more viscous and less mobile with increasing SiO_2 content, and felsic magma tends to cause explosive eruptions. Magma usually contains not only SiO_2 but also several percent of alkali and alkaline-earth metal oxides, including Na_2O, K_2O, MgO, and CaO. Hence, examining the effects of metal oxides on the physicochemical properties of magma at high pressure allows us to understand magmatic processes in a precise manner. Among many properties, high-pressure sound velocity is crucial because the sound velocity data of silicate melts bring us direct information for understanding the detailed structure of the Earth's interior combined with seismological data. Structural investigation of silicate glasses which are quenched from melts is useful to obtain insights into deep magmatism because of the structural similarity between the strong network-forming silicate glasses and silicate melts (Price et al. 1988; Susman et al. 1990; Elliott 1992; Hennet et al. 2007) and the experimental difficulty of melts under pressure. A large number of sound velocity data of silica glass have been reported (Kondo et al. 1981; Schroeder et al. 1990; Suito et al. 1992; Polian and Grimsditch 1993; Yokoyama et al. 2010). In addition to these previous studies on SiO_2 glass, the sound velocity of complex systems, such as an aluminosilicate glass containing various cations, should be investigated further because each cation possibly plays an individual role and affects the physical properties of the glass differently.

Electronic supplementary material The online version of this article (https://doi.org/10.1007/s00269-020-01098-3) contains supplementary material, which is available to authorized users.

✉ Koji Aoki
koji.aoki.t5@dc.tohoku.ac.jp

[1] Division of Earth and Planetary Materials Science, Faculty of Science, Tohoku University, Sendai 980-8578, Japan

[2] Department of Earth and Planetary Materials Science, Graduate School of Science, Tohoku University, Sendai 980-8578, Japan

Generally, the cations in a silicate melt/glass are divided into network-forming cations (e.g., Si^{4+} and Al^{3+}) and network-modifying cations (e.g., Mg^{2+}, Ca^{2+}, Na^{+}, and K^{+}) (Mysen 1988). The network formers in silicate glasses and melts correspond to a tetrahedral cation (T), which constitutes a $[TO_4]$ tetrahedron as the basic unit of the silicate network. The network modifiers cut the linkages between adjacent $[TO_4]$ tetrahedra and create two non-bridging oxygens (NBOs) (Mysen et al. 1982). The ratio of network formers to modifiers represents the degree of polymerization of a silicate network, which is usually indicated by the NBO/T ratio given as $NBO/T = (2O - 4T)/T$ (Mysen et al. 1981). The NBO/T values of natural magmas range between 0 and 2 (Whittington et al. 2000).

There is a major difference between the $[AlO_4]^{5-}$ and $[SiO_4]^{4-}$ tetrahedral network-forming units. The $[AlO_4]^{5-}$ tetrahedron contains one negative charge, whereas each $[SiO_4]^{4-}$ tetrahedron is electrically neutral. Because the $[AlO_4]^{5-}$ tetrahedron acts as a network-forming unit, the $[AlO_4]^{5-}$ charge needs should be compensated using alkali and alkaline-earth cations or a tricluster oxygen (Stebbins and Xu 1997; Xiang et al. 2013). Thus, Al^{3+} acts as a network-former cation if sufficient charge compensating cations (e.g., alkali and alkaline-earth cations) are available in a silicate glass. The tendency of modifying cations to balance the charge of the $[AlO_4]^{5-}$ units decreases with increasing field strength (ratio of the charge to the square radius), i.e., $K^{+} < Na^{+} < Ca^{2+} < Mg^{2+}$ (Mysen 1987). Here, the alkali and alkaline-earth cations can occupy both the sites in aluminosilicate systems as a modifier and a charge compensator (Taylor and Brown 1979; Navrotsky et al. 1982; McMillan 1984; Domine and Piriou 1986). The interaction between the charge compensating cations and the $[AlO_4]^{5-}$ units is more ionic and stronger than that between the cations and NBO (Uchino et al. 1993). The effect of the existence of two such types of cation sites on the properties of aluminosilicate glass can be referred to as the "mixed site effect" (Xiang et al. 2013).

Previous studies have investigated the influence of the presence of network-modifying cations on the physical properties and structures of aluminosilicate (Allwardt et al. 2005a, b; Lin and Liu 2006; Allwardt et al. 2007; Xiang et al. 2013). According to the nuclear magnetic resonance (NMR) studies (Allwardt et al. 2005a, b, 2007), the physical properties, including the density and viscosity, of the aluminosilicate glasses under pressure differ considerably depending on the type of the network-modifying cations. For example, the densities of the alkaline-earth aluminosilicate glasses ($Ca_3Al_2Si_6O_{18}$ and $Ca_{1.5}Mg_{1.5}Al_2Si_6O_{18}$) are more likely to drastically increase at an elevated pressure than those of the alkali aluminosilicate glasses ($K_3AlSi_3O_9$ and $Na_3AlSi_3O_9$) because of the higher compressibility. Thus, the physical properties of the aluminosilicate glasses are strongly dependent on the constitutive metal cations (Allwardt et al. 2005a).

In addition, Brillouin and Raman scattering spectroscopy experiments have indicated that alkali cations affect the bulk and shear modulus; however, the alkaline-earth cations considerably influence only the shear modulus at the ambient pressure (Lin and Liu 2006; Weigel et al. 2016). As an explanation for this trend, Lin and Liu (2006) denoted that the alkaline-earth modifier cations prefer to associate with the depolymerized anionic structure of silicate glass, such as $Si_2O_7^{6-}$ (dimer) and $Si_2O_6^{4-}$ (chain), rather than the more polymerized $Si_2O_5^{2-}$ (sheet) and SiO_2. Because the latter two units mainly control the compression behaviors, the presence of an alkaline-earth cation exhibits only a minor relation with the bulk modulus.

In this study, we focused on the sound velocities of the following four types of aluminosilicate glass: $Mg_3Al_2Si_6O_{18}$ (MAS), $Ca_3Al_2Si_6O_{18}$ (CAS), $Na_3AlSi_3O_9$ (NAS), and $K_3AlSi_3O_9$ (KAS). The glass compositions were determined using a simple mafic magma model, and an NBO/T ratio of 0.5 at ambient pressure was used for all the samples. Further, we investigated the velocities under high pressure using a pulse-echo overlap ultrasonic technique to understand the pressure dependences and effects of the network-modifying cations on the elastic properties of the aluminum silicate glass.

Experimental procedure

The starting materials were prepared using reagent-grade MgO, $CaCO_3$, Na_2CO_3, K_2CO_3, Al_2O_3, and SiO_2. The oxides and carbonates were dried for a day at 1000 °C and 200 °C, respectively. After drying, the powders were weighed in the desired proportions and mixed in an agate mortar with acetone for 1 h. Each mixed powder was melted in a Pt–Rh crucible at 1400 °C for 10 h and subsequently quenched to produce the glasses.

The sound velocity measurements were performed under high pressure using the pulse-echo overlap technique. To generate high pressures, a 3000-ton Kawai-type multi-anvil apparatus installed in Tohoku University was used. A schematic illustration of the high-pressure cell assembly is presented in Fig. 1. A fully densified alumina cylinder below the sample was used as a buffer rod. A NaCl cup was placed around the sample to reduce the deviatoric stresses. The top and bottom faces of the sample, the alumina buffer rod, and the two diagonally truncated edge faces of a tungsten carbide anvil were mirror-polished using a 1-μm diamond paste to ensure smooth propagation of the ultrasonic waves. A 10°-rotated Y-cut $LiNbO_3$ transducer was bonded to the polished truncated edge face of the anvil with epoxy resin. The P- and S-wave signals reflected from the interface of

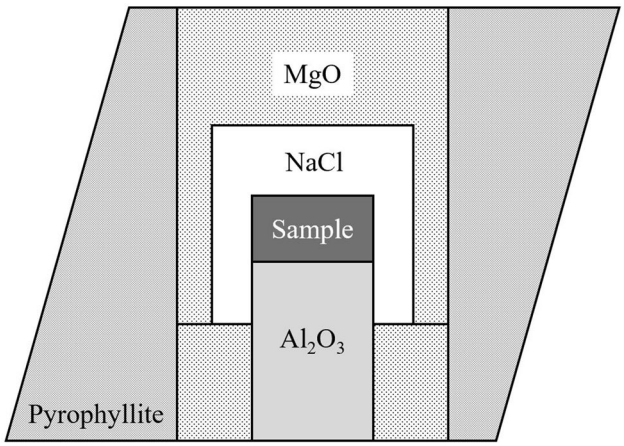

Fig. 1 Schematic of high-pressure cell assembly (cross-sectional view)

the buffer rod and the sample and the bottom of the sample were acquired using a digital oscilloscope. A typical signal is illustrated in Fig. 2. The sampling rate for collecting the signals was 5.0×10^9 point/s. Details of the ultrasonic measurements considered in this study are described in Higo et al. (2006).

Pressure was estimated using the relation between the pressure in the cell assembly and the load of the press calibrated by the bismuth transitions: Bi(I)–Bi(II) transition at 2.55 GPa and Bi(III)–Bi(V) transition at 7.7 GPa (Bean et al. 1986). The sample length at each pressure condition was calculated using Cook's method (Cook 1957). The details of the used method are described in Suito et al. (1992). In this method, the sample length under pressure is calculated using the zero-pressure density (ρ_0), initial sample length (l_0), and travel time of the compressional and shear waves of the sample. ρ_0 was obtained using Archimedes' principle by considering pure water as the immersion liquid at room temperature. The densities of the MAS, CAS, NAS, and KAS glasses were 2.53(3), 2.652(1), 2.39(4), and 2.35(2) g/cm^3, respectively. Although the application of the Cook's method is based on a critical assumption that sample is compressed fully elastically, the sample length of the four glasses was shortened by approximate 1–2% after the experiments. This implies that samples did not show perfect elasticity. Here, we also calculated the length of samples under high pressure assuming that the linearity between initial and recovered sample length is established. The difference in calculated velocity between Cook's method and linear assumption is less than 0.05 km/s, and we confirmed that our length estimation can be usable for the velocity calculation under high pressure.

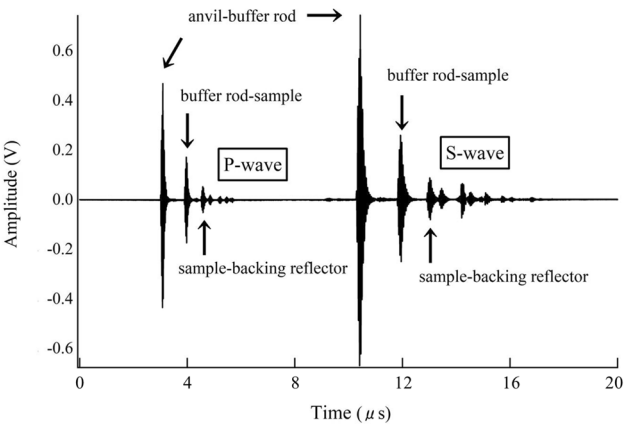

Fig. 2 Typical waveform data of the $Ca_3Al_2Si_6O_{18}$ glass at 2.7 GPa. Each echo of the P- and S-waves from the buffer rod sample and the sample-backing plate boundaries are clearly shown. The two-way travel time corresponds to the time difference between two echoes

Results and discussion

The sound velocity measurements of the four types of aluminosilicate glasses were conducted at high pressures up to 7.8 GPa. All the experimental results are summarized in Supplementary Table 1. The measured compressional wave velocity (V_P) and shear wave velocity (V_S) of the samples as a function of pressure are shown in Figs. 3 and 4, respectively. The velocity of the MAS glass was the highest throughout the experimental range, followed, in order, by those of the CAS, NAS, and KAS glasses. The pressure dependence of the V_P and V_S for the MAS glass changed from negative to positive at approximately 2 GPa; subsequently, the velocities increased linearly with pressure. With

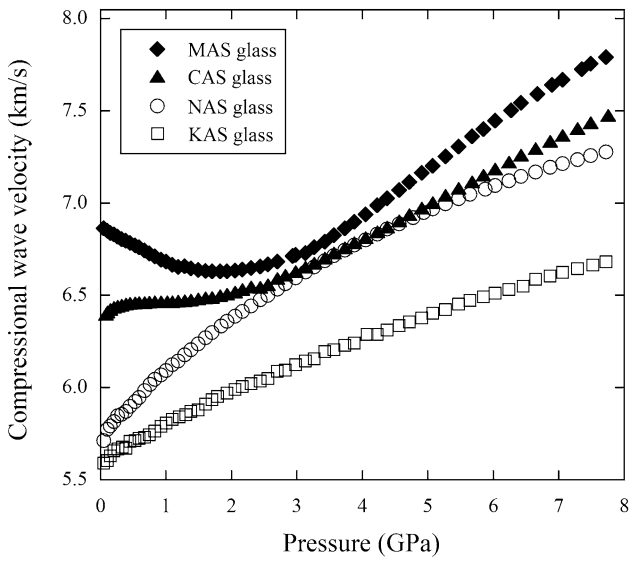

Fig. 3 Compressional wave velocities of the four aluminosilicate glasses as a function of pressure

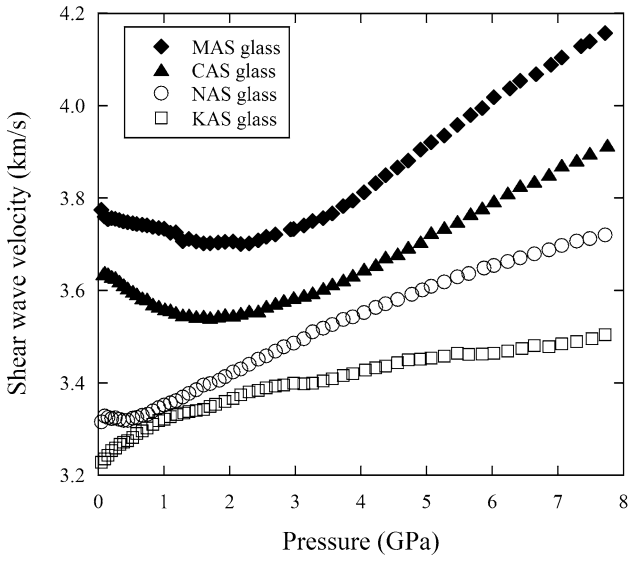

Fig. 4 Shear wave velocities of the four aluminosilicate glasses as a function of pressure

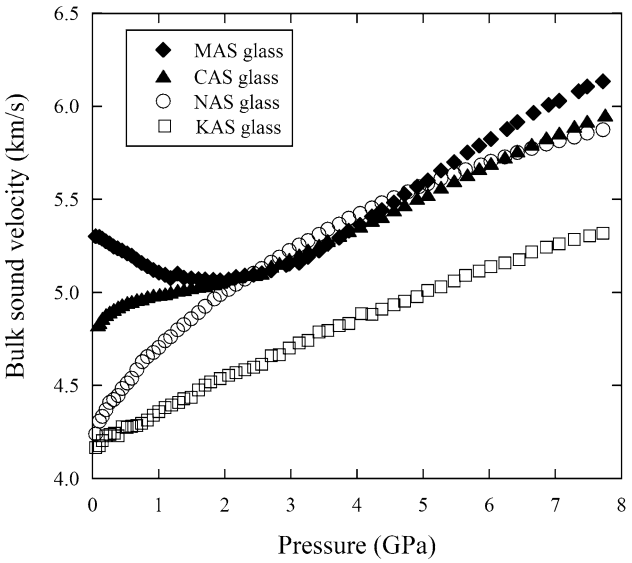

Fig. 5 Bulk wave velocities of the four aluminosilicate glasses as a function of pressure

respect to the pressure behavior of V_P, only the MAS glass exhibited the minimum value at approximately 2 GPa. In case of the CAS glass, the pressure dependence of velocity changed at approximately 2 GPa. Below 2 GPa, the V_P of the CAS glass slightly increased, whereas V_S decreased with compression. In contrast to the high-pressure behavior of the V_P and V_S for the MAS and CAS glasses, the sound velocities of the NAS and KAS glasses showed a relatively monotonic increase with pressure. With respect to the NAS glass, V_P largely increased over the low-pressure range but the graphed slope (V_P vs. pressure) gradually flattened with increasing pressure (Fig. 3). In contrast, the V_S of the NAS glass had a minimum at approximately 0.5 GPa but subsequently increased with increasing pressure. In the case of the KAS glass, the sound velocities exhibited tendencies similar to that of the NAS glass. Both V_P and V_S continued to increase and were less sensitive to pressure when compared with the NAS glass.

The bulk sound velocity (V_B) was calculated based on the compressional and shear velocities using the following equation:

$$V_B = \sqrt{V_P^2 - \frac{4}{3}V_S^2} = \sqrt{\frac{K_S}{\rho}} \quad (1)$$

where K_S is the adiabatic bulk modulus and ρ is the density. The pressure dependence of V_B is presented in Fig. 5. It exhibited a tendency similar to that of V_P. The pressure behavior of V_B and V_P for the MAS and CAS glasses clearly changed at approximately 2 GPa, and the V_B of the NAS and KAS glasses increased monotonically with compression. Considering the quantitative values of the velocities, interestingly, the V_P and V_B of the MAS, CAS, and NAS glasses are similar, while those of the KAS glass are markedly different. V_P and V_B of KAS glass are approximately 1 km/s smaller than those of the other three glasses.

Using sound velocities in the current study, Poisson's ratio (σ) was also obtained by the following equation:

$$\sigma = \frac{V_P^2 - 2V_S^2}{2(V_P^2 - V_S^2)}. \quad (2)$$

Poisson's ratio represents an ease to elastic deformation and it approximately falls in 0.1 to 0.5 for various materials. Pressure dependence of Poisson's ratio for the four glasses is also shown in Fig. 6. In terms of Poisson's ratio of the four glasses above 3 GPa, NAS glass was the largest, followed by CAS, KAS, and MAS in this order.

Although Poisson's ratio of CAS, NAS, and KAS glasses had positive pressure dependence, Poisson's ratio of MAS glass behaved anomalously; it declined below 1 GPa and then it was almost stagnant up to 2 GPa. Poisson's ratio of CAS glass largely increased below 1 GPa and gently increased above 1 GPa. Considering NAS glass, the degree of the change of Poisson's ratio value was the largest in this pressure range. It largely increased up to 2 GPa and the degree of increase became gradual. Poisson's ratio of KAS glass increased monotonically. Pressure dependence of Poisson's ratio of MAS, CAS, and NAS glasses showed similar inclination above 2 GPa though that of KAS glass was steeper when compared with other glasses.

The high-pressure sound velocity systematics for a range of silicate glass compositions up to 10 GPa is listed in Table 1. The pressure evolution of the sound velocities of silicate glasses in the pressure range of approximately 0–10 GPa can be broadly classified into two groups based

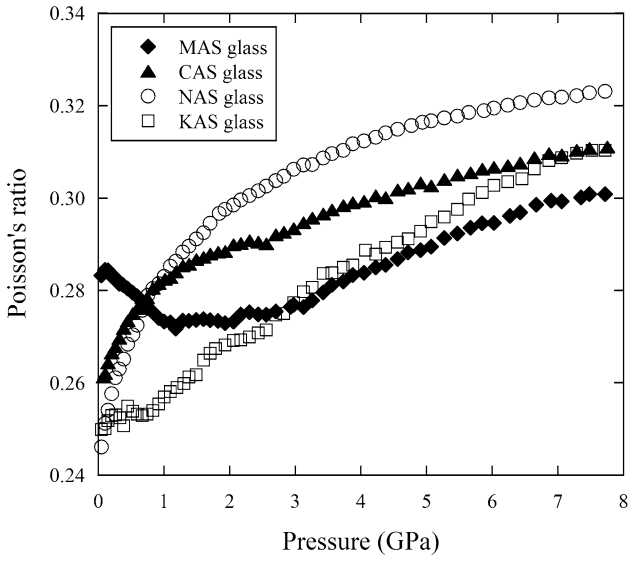

Fig. 6 Poisson's ratio of the four aluminosilicate glasses as a function of pressure

on the degree of polymerization (Sakamaki et al. 2014). One group is characterized by fully polymerized glass, such as silica (SiO_2), albite ($NaAlSi_3O_8$), and jadeite ($NaAlSi_2O_6$) glasses (NBO/T = 0). It exhibits a minimum in the pressure dependence of sound velocities at a few gigapascals (Suito et al. 1992; Zha et al. 1994; Sanchez-Valle and Bass 2010; Sakamaki et al. 2014). In the current study, the MAS and CAS glasses would belong to this group. The other group is characterized by depolymerized glass, such as enstatite ($MgSiO_3$), and diopside ($CaMgSi_2O_6$) glasses (NBO/Si = 2.0). It usually exhibits a monotonic increase in V_P with pressure (Sanchez-Valle and Bass 2010; Sakamaki et al. 2014).

The difference in the pressure dependence of V_P and V_S with respect to the polymerized and depolymerized glasses can be attributed to the variation in the pressure-induced structural changes and the amount of free volume, which is the space not occupied by [AlO_X] polyhedra or other cations in the network structure (Zha et al. 1994; Lin and Liu 2006; Yokoyama et al. 2010; Sakamaki et al. 2014; Clark et al. 2016; Moulton et al. 2019). Silicate glass is a structurally disordered material. The large number of rings composed of approximately 3–10 [TO_4] tetrahedra creates three-dimensional construction. The intermediate-range order (IRO) is generally considered to be the longest order in silicate glass (Renou et al. 2017) and it corresponds to the ring's properties (T–T distribution and the inter-tetrahedral angle). Owing to the amorphous nature of glass, free volume can also be observed between rings of various sizes because of the connectivity of the corner shearing [TO_4] tetrahedra (Kohara et al. 2011; Renou et al. 2017). The quantity of free

Table 1 Summary of the transition of pressure dependence of V_P and V_S for silicate glasses in the pressure range of approximately 0–10 GPa

Composition	$\frac{\partial V_P}{\partial P}$	Transition pressure of V_P behavior	$\frac{\partial V_S}{\partial P}$	Transition pressure of V_S behavior
NBO/T = 0 at 1 atm				
Jadeite ($NaAlSi_2O_6$)[1]	− +	6 GPa	− +	7 GPa
Albite ($NaAlSi_3O_8$)[1]	− +	6 GPa	− ~ 0	6 GPa
Anorthite ($CaAl_2Si_2O_8$)[2]	− +	6 GPa	No data	No data
NBO/T = 0.5 at 1 atm				
MAS ($Mg_3Al_2Si_6O_{18}$)	− +	2 GPa	− +	2 GPa
CAS ($Ca_3Al_2Si_6O_{18}$)	~ 0 +	2 GPa	− +	2 GPa
NAS ($Na_3AlSi_3O_9$)	+		− +	0.5 GPa
KAS ($K_3AlSi_3O_9$)	+		+	
NBO/T = 0.6 at 1 atm				
BCR-2 Basalt[3]	− +	4.5 GPa	− +	4.5 GPa
NBO/T = 0.8 at 1 atm				
BIR-1 Basalt[4]	− +	1.2 GPa	− +	1.2 GPa
NBO/T = 2.0 at 1 atm				
Enstatite ($MgSiO_3$)[5]	+		− +	8 GPa
Diopside ($CaMgSi_2O_6$)[1]	+		− ~ 0	1.5 GPa

[1]Sakamaki et al. (2014)
[2]Moulton et al. (2019)
[3]Clark et al. (2016)
[4]Liu and Lin (2014)
[5]Sanchez-Valle and Bass (2010)

volume in silicate glasses is considerably affected by their degree of polymerization. Polymerized glass contains more free volumes than depolymerized glass because network-modifying cations cause a collapse of three-dimensional network structures. In fact, reverse Monte Carlo modeling revealed that fully polymerized silica glass contained 31.9% voids at ambient pressure and depolymerized enstatite glass (NBO/Si = 2.0) included only 2.6% free volume because of large numbers of edge-shared [MgO_X] polyhedra (Kohara et al. 2011). The pressure dependence of sound velocities of these two glasses distinctly differ to each other (Zha et al. 1994; Sanchez-Valle and Bass 2010). The velocities of silica glass abruptly change in slope of the velocity–pressure profiles (Zha et al. 1994). On the other hand, a computational study revealed that both V_P and V_S of enstatite glass increase monotonically with pressure (Ghosh et al. 2014) though experimental sound-velocity measurement of enstatite glass using Brillouin spectroscopy showed gradual decrease in the V_S up to 8 GPa (Sanchez-Valle and Bass 2010). This difference resulted from the frequency dependence of the bulk modulus. Brillouin spectroscopy measures the unrelaxed bulk modulus whereas Ghosh et al. (2014) used the relaxed bulk modulus for the calculation of the velocity.

Pressure-induced structural transitions of various silicate glasses have been reported based on X-ray diffraction (Sakamaki et al. 2014; Drewitt et al. 2015) and NMR analysis (Stebbins et al. 2013). Shrinkage of the IRO is mainly caused by the reduction and collapse of free volume through the rearrangement of the Si–O–Si bond angles rather than bond shortening. The topological rearrangement continues until short-range repulsive forces in the structure become sufficiently large to prevent any further collapse. The rearrangement transforms the glass into more densely packed structure (Dove 1997). In other words, especially at lower pressure range, compressional processes of silicate glasses are strongly dependent on their degree of polymerization. Polymerized glasses are more sensitive to compression than depolymerized glasses and its dominant mechanism is reduction of free volumes.

The different pressure dependence of sound velocity between polymerized and depolymerized glasses can be also explained by the variety of atomic-scale structural change: i.e., significant modifications in the local structure and topology of the [TO_4] networks resulting from the ring closure and the collapse of interstitial free volume (Sanchez-Valle and Bass 2010; Liu and Lin 2014; Sakamaki et al. 2014; Clark et al. 2016). The velocity reduction showed not only general polymerized glasses, but also our MAS and CAS glasses would correlate with huge shrinkage of IRO in the lower pressure range. The collapse of free volumes caused by topological rearrangement is interpreted as an origin of elastic softening associated with the decrease of elastic moduli of glasses with pressure. The elastic softening and velocity decreasing are essentially identical in terms of the structural changes. The previous computational study of anorthite ($CaAl_2Si_2O_8$) glass (NBO/T = 0) showed non-monotonic pressure evolution of the sound velocities up to 155 GPa (Ghosh and Karki 2018). From 0 to 10 GPa, the V_P and V_B of anorthite glass showed monotonic increase with pressure and V_S displayed initial drop in its magnitude around 5 GPa and increased thereafter. These results were actually consistent with the measured behavior of the CAS glass in the current study. Ghosh and Karki also interpreted the origin of this velocity reduction as the topological rearrangement of the network-forming tetrahedra. Hence, the measured velocity decreases of MAS and CAS glasses at 2 GPa are thought to be caused by the shrinkage of free volume.

Recently, depolymerized basalt glasses have been reported to exhibit a minimum value with respect to their sound velocities with compression (BIR-1 basalt glass; Liu and Lin 2014; BCR-2 basalt glass; Clark et al. 2016). The NBO/T values of these glasses were 0.8 and 0.6, respectively. Clark et al. (2016) interpreted the softening of the V_P and V_S of the BCR-2 basalt glass as topological rearrangement in the aluminosilicate network. The silicate network is still sufficiently interconnected to cause a reduction of free volume. Generally, the pressure-induced reduction of sound velocities in aluminosilicate glasses at a few gigapascals is closely related to the presence of compressional void spaces in the structures. Velocity reduction is expected to occur universally in aluminosilicate glasses at low pressure and independent of the degree of polymerization if compressible free volumes are present.

Considering the correlation between the degree of polymerization and the reduction of velocities, the sound velocities of all the glasses in this study would denote softening under pressure because the NBO/T value of all the glasses calculated from their chemical composition was 0.5. However, the sound velocities of each type of glass exhibited different pressure-induced changes, which can be attributed to the different properties of cations in aluminosilicate glasses, including the ionic radii and field strength. The radius of each modifier cation is $Mg^{2+} < Ca^{2+} \approx Na^{+} < K^{+}$ (Shannon 1976) by assuming that the coordination numbers are 5, ~ 6–7, ~ 6–7, and ~ 8–11, respectively (Jackson et al. 1987; Okuno and Marumo 1993; George and Stebbins 1996; Cormier and Neuville 2004; Neuville et al. 2004; Shimoda et al. 2007; Guignard and Cormier 2008). The larger the modifying cation, the greater will be the resistance to the shrinkage of tetrahedral networks of silicate glass during compression (Shimoda et al. 2005). In addition, pressure-induced behavior of cation–anion bond distances depends on whether glasses contain Al or not. The Si–O bond distance in the silicate glasses/melts is known to show an initial increase (Funamori et al. 2004; Sato and Funamori 2010;

Sun et al. 2011; Ghosh et al. 2014). However, in the case of aluminosilicate glasses, computational studies of anorthite glass showed that Si–O bond distance remains almost constant whereas Al–O bond length increases with pressure in a range of 0–10 GPa (Ghosh and Karki 2018). In terms of structural evolution, Ghosh and Karki interpreted that the little change of Si–O length is correlated with topological rearrangement of [TO_4] tetrahedra. The increase of Al–O length corresponds to the Al–O coordination number increase. The Si–O coordination number also displays little change with pressure, and this change means negligible effect of compression on the Si–O network up to 10 GPa. In short, Al–O coordination number preferentially increases in the pressure range. This local environment of Al in aluminosilicate glass under compression is strongly influenced by the cation field strength of modifier cations. According to an NMR analysis for the three aluminosilicate glasses with the same composition as CAS, NAS, and KAS glasses used in this study, the higher cation field strength (Ca > Na > K) yields more highly coordinated Al (Allwardt et al. 2005b). Moreover, the average Al coordination of CAS, NAS, and KAS glasses were remarkably correlated with the density under pressure. This implies that the densification mechanism for aluminosilicate glasses is closely related to the increase in the Al–O coordination number. Especially in the low pressure around 5 GPa, density is also substantially impacted by the cation field strength and increases in the following order: CAS > NAS > KAS. Although the noticeable increase in Al–O coordination number showed in the NMR analysis is not expected in the current four glasses due to the cold compression, the difference in pressure evolution of velocities may be caused by different sensitivity of Al coordination to pressure between the above three composition. In view of the cation field strength, the MAS composition glass should contain more highly coordinated Al and have more dense structure than the CAS composition.

Therefore, in this study, the density of the MAS glass containing Mg^{2+} was more likely to increase than that of the remaining glasses. The effects of the cation field strength on the structure and elastic properties of the aluminosilicate glasses should be noted. The tendency to compensate the negatively charged $[AlO_4]^{5-}$ units decreases with increasing field strength: $^{[\sim 8-11]}K^+ < ^{[\sim 6-7]}Na^+ < ^{[\sim 6-7]}Ca^{2+} < ^{[5]}Mg^{2+}$ (Mysen 1987). Given that all Al is fourfold-coordinated, Al^{3+} forms tricluster units and simultaneous NBO. These connection forms are unstable due to the high field strength of the modifying cations, such as Mg^{2+} and Ca^{2+}, in the aluminosilicate glass network (Stebbins and Xu 1997). With respect to the glasses in this study, the degree of polymerization and compressibility increased in the order of MAS, CAS, NAS, and KAS (Kuryaeva 2012). The pressure behavior of the sound velocities of each type of glass in this study varied because of the structural and topological differences caused by the properties of the modifying cations and was strongly dependent on the kind of cation, especially in the low-pressure range (< 2 GPa). The elastic moduli of aluminosilicate glasses at ambient pressure increase with the increasing field strength of the modifying cations (Lin and Liu 2006; Weigel et al. 2016). This is consistent with our measured V_P and V_S values at ambient pressure. The different changes in the sound velocities of each aluminosilicate glass with pressure, shown in Figs. 4 and 5, indicate that the increasing degree of elastic moduli is strongly influenced by the field strength of the modifying cation; further, the higher the field strength of the modifying cation, the lower will be the increase in the elastic moduli of the aluminosilicate glasses, especially in the low-pressure range (< 2 GPa). This assumes that the collapse and resulting reduction of free volume are dominant rather than the compression of cation sites in this pressure range. Therefore, the NAS and KAS glasses in this study showed greater elastic behavior rather than softening because of the size and low field strength of the modifier cations. The collapse of the remaining void space and the high field strength of the modifying cation could be considered responsible for the softening of the MAS and CAS glasses.

The absolute values of the measured velocity for the MAS, CAS, NAS, and KAS glasses were considerably different from each other. Especially the V_P and V_B of KAS glass were much lower than those of the other glasses. Previous studies for silicate glasses have also revealed that the absolute value of high-pressure sound velocities was divided into two groups by its magnitude (Sakamaki et al. 2014; Clark et al. 2016). For instances, the glasses in high- V_P group displays V_P greater than 6.4 km/s and that of the other groups is lower than 6.2 km/s. In most cases, this classification corresponds to the degree of polymerization of silicate glasses. Polymerized and depolymerized glasses belong to the low- and high-velocity groups, respectively. However, Moulton et al. (2019) showed that the V_P of the fully polymerized anorthite glass is more than approximate 6.6 km/s, closer in magnitude to diopside glass than to polymerized glasses such as albite glass. Moulton et al. (2019) proposed that introducing of the concept of the fragility (Angell 1985) of the composition, rather than polymerization for better understanding of the high-pressure V_P values of silicate glasses. The fragility value for anorthite, diopside, and albite glasses are 54, 57, and 26, respectively (Russell and Giordano 2005). In short, it is suggested that the sound velocity value of silicate glasses may become higher with increase of their fragility. In general, the fragility of silicate melts is strongly related with the connectivity of silicate network and the strength of T–O–T bonds (Yue and Christiansen 1999). The strong melts have the well-developed structure with a high connectivity of network. By contrast, fragile melts possess the weak structure with a low connectivity

of network and more ionic bonds. The difference of cation field strength causes the variation of network connectivity, i.e., the fragility of silicate glasses. This is attributed to the fact that the T–O–T bond is weakened more easily by Mg^{2+} or Ca^{2+} than by Na^{+} and K^{+} because the bonding between Mg^{2+} or Ca^{2+} and bridging-oxygen (BO) is stronger than that between Na^{+} or K^{+} and BO (Yue and Christiansen 1999). This difference of fragility may correlate with the diversity of measured velocity values of the four glasses though a much larger database of silicate compositions is needed to make more quantitative discussion.

Our results prove that the elastic properties of aluminosilicate glasses having the same degree of polymerization are strongly affected by the size and field strength of the modifying metal cations. Metal cations mainly control the compressional processes at low pressure; hence, the sound velocities of the aluminosilicate glasses largely differ depending on the variety of the modifying metal cations.

Conclusion

The pressure behaviors of the sound velocities of the aluminosilicate glasses are considerably influenced by the modifying cations. The pressure dependence of the sound velocities of the alkaline-earth aluminosilicate glasses clearly change at 2 GPa, whereas those of the alkali aluminosilicate glasses increase monotonically with compression. This contrast can be attributed to the differences in the size and field strength of the modifying cations because the presence of free volume and NBO in the aluminosilicate networks (the factors that mainly control the elastic properties of aluminosilicates) are considerably affected by the properties of the modifying cations. The various types of metal cations in aluminosilicate glass yield a variety of sound velocities when these glasses are subjected to pressure.

Acknowledgement The authors would like to thank Y. Higo, N. Hisano, Y. Horioka, and M. Goto for their support of the experiments. The authors would also like to thank Enago (www.enago.jp) for the English language review. This research was performed with the support of JSPS KAKENHI Grant Numbers JP15H05828, JP17H04860, JP17K18797, JP19H01985, and JP19K21890.

References

Allwardt JR, Poe BT, Stebbins JF (2005a) The effect of fictive temperature on Al coordination in high-pressure (10 GPa) sodium aluminosilicate glasses. Am Mineral 90:1453–1457. https://doi.org/10.2138/am.2005.1736

Allwardt JR, Stebbins JF, Schmidt BC, Frost DJ, Withers AC, Hirschmann MM (2005b) Aluminum coordination and the densification of high-pressure aluminosilicate glasses. Am Mineral 90:1218–1222. https://doi.org/10.2138/am.2005.1836

Allwardt JR, Stebbins JF, Terasaki H, Du L-S, Frost DJ, Withers AC, Hirschmann MM, Suzuki A, Ohtani E (2007) Effect of structural transitions on properties of high-pressure silicate melts: ^{27}Al NMR, glass densities, and melt viscosities. Am Mineral 92:1093–1104. https://doi.org/10.2138/am.2007.2530

Angell CA (1985) Spectroscopy simulation and scattering, and the medium range order problem in glass. J Non-Cryst Solids 73:1–17. https://doi.org/10.1016/0022-3093(85)90334-5

Bean VE, Akimoto S, Bell PM, Block S, Holzapfel WB, Manghnani MH, Nicol MF, Stishov SM (1986) Another step toward an international practical pressure scale: 2nd AIRAPT IPPS task group report. Physica B+C 139–140:52–54. https://doi.org/10.1016/0378-4363(86)90521-8

Clark AN, Lesher CE, Jacobsen SD, Wang Y (2016) Anomalous density and elastic properties of basalt at high pressure: reevaluating of the effect of melt fraction on seismic velocity in the Earth's crust and upper mantle. J Geophys Res Solid Earth 121:4232–4248. https://doi.org/10.1002/2016JB012973

Cook RK (1957) Variation of elastic constants and static strains with hydrostatic pressure: a method for calculation from ultrasonic measurements. J Acoust Soc Am 29:445–449. https://doi.org/10.1121/1.1908922

Cormier L, Neuville DR (2004) Ca and Na environments in Na_2O–CaO–Al_2O_3–SiO_2 glasses: influence of cation mixing and cation–network interactions. Chem Geol 213:103–113. https://doi.org/10.1016/j.chemgeo.2004.08.049

Domine F, Piriou B (1986) Raman spectroscopic study of the SiO_2–Al_2O_3–K_2O vitreous system; distribution of silicon second neighbors. Am Mineral 71:38–50. https://pubs.geoscienceworld.org/ammin/article-abstract/71/1-2/38/41805/Raman-spectroscopic-study-of-the-SiO2-Al2O3-K2O

Dove MT (1997) Theory of displacive phase transitions in minerals. Am Mineral 82:213–244. https://doi.org/10.2138/am-1997-3-401

Drewitt JWE, Jahn S, Sanloup C, de Grouchy C, Garbarino G, Hennet L (2015) Development of chemical and topological structure in aluminosilicate liquids and glasses at high pressure. J Phys: Condens Matter 27:105103. https://doi.org/10.1088/0953-8984/27/10/105103

Elliott SR (1992) The origin of the first sharp diffraction peak in the structure factor of covalent glasses and liquids. J Phys: Condens Matter 4:7661–7678. https://doi.org/10.1088/0953-8984/4/38/003

Funamori N, Yamamoto S, Yagi T, Kikegawa T (2004) Exploratory studies of silicate melt structure at high pressures and temperatures by in situ X-ray diffraction. J Geophys Res 109:B03203. https://doi.org/10.1029/2003JB002650

George AM, Stebbins JF (1996) Dynamics of Na in sodium aluminosilicate glasses and liquids. Phys Chem Miner 23:526–534. https://doi.org/10.1007/BF00242002

Ghosh DB, Karki BB (2018) First-principles molecular dynamics simulations of anorthite ($CaAl_2Si_2O_8$) glass at high pressure. Phys Chem Minerals 45:575–587. https://doi.org/10.1007/s00269-018-0943-4

Ghosh DB, Karki BB, Stixrude L (2014) First-principles molecular dynamics simulations of $MgSiO_3$ glass: structure, density, and elasticity at high pressure. Am Mineral 99:1304–1314. https://doi.org/10.2138/am.2014.4631

Guignard M, Cormier L (2008) Environments of Mg and Al in MgO–Al_2O_3–SiO_2 glasses: a study coupling neutron and X-ray diffraction and Reverse Monte Carlo modeling. Chem Geol 256:111–118. https://doi.org/10.1016/j.chemgeo.2008.06.008

Hennet L, Pozdnyakova I, Cristiglio V, Cuello GJ, Jahn S, Krishnan S, Sabougni M-L, Price DL (2007) Short- and intermediate-range order in levitated liquid aluminates. J Phys: Condens Matter 19:455210. https://doi.org/10.1088/0953-8984/19/45/455210

Higo Y, Inoue T, Li B, Irifune T, Liebermann RC (2006) The effect of iron on the elastic properties of ringwoodite at high pressure.

Phys Earth Planet Inter 159:276–285. https://doi.org/10.1016/j.pepi.2006.08.004

Jackson WE, Brown GE, Ponader CW (1987) X-ray absorption study of the potassium coordination environment in glasses from the $NaAlSi_3O_8$-$KAlSi_3O_8$ binary: structural implications for the mixed-alkali effect. J Non-Cryst Solids 93:311–322. https://doi.org/10.1016/S0022-3093(87)80177-1

Kohara S, Akola J, Morita H, Suzuya K, Weber JKR, Wilding MC, Benmore CJ (2011) Relationship between topological order and glass forming ability in densely packed enstatite and forsterite composition glasses. Proc Natl Acad Sci 108:14780–14785. https://doi.org/10.1073/pnas.1104692108

Kondo K, Iio S, Sawaoka A (1981) Nonlinear pressure dependence of the elastic moduli of fused quartz up to 3 GPa. J Appl Phys 52:2826–2831. https://doi.org/10.1063/1.329012

Kuryaeva RG (2012) Effect of alkali cations on the compressibility of $MAlSi_3O_8$ glasses (M=Na, K, Rb, Cs) in the pressure range up to 6.0 GPa. Phys Chem Glas 53:8. https://www.researchgate.net/publication/263385312

Lin C-C, Liu L (2006) Composition dependence of elasticity in aluminosilicate glasses. Phys Chem Miner 33:332–346. https://doi.org/10.1007/s00269-006-0084-z

Liu J, Lin J-F (2014) Abnormal acoustic wave velocities in basaltic and (Fe, Al)-bearing silicate glasses at high pressures. Geophys Res Lett 41:8832–8839. https://doi.org/10.1002/2014GL062053

McMillan P (1984) A Raman spectroscopic study of glasses in the system CaO–MgO–SiO_2. Am Mineral 69:645–659. http://www.minsocam.org/ammin/AM69/AM69_645.pdf

Moulton BJA, Henderson GS, Martinet C, Martinez V, Sonneville C, de Ligny D (2019) Structure—longitudinal sound velocity relationships in glassy anorthite ($CaAlSi_2O_8$) up to 20 GPa: an in situ Raman and Brillouin spectroscopy study. Geochim Cosmochim Acta 261:132–144. https://doi.org/10.1016/j.gca.2019.06.047

Mysen BO (1987) Magmatic silicate melts: relations between bulk composition, structure and properties. In: Mysen BO (ed) Magmatic processes: physicochemical principles. The Geochemical Society, Penn, pp 375–399

Mysen BO (1988) Structure and properties of silicate melts. Elsevier, Amsterdam

Mysen BO, Virgo D, Kushiro I (1981) The structure role of aluminum in silicate melts—a Raman spectroscopic study at 1 atmosphere. Am Mineral 66:678–701. http://www.minsocam.org/ammin/AM66/AM66_678.pdf

Mysen BO, Virgo D, Seifert FA (1982) The structure of silicate melts: implications for chemical and physical properties of natural magma. Rev Geophys 20:353–383. https://doi.org/10.1029/RG020i003p00353

Navrotsky A, Peraudeau G, McMillan P, Coutures J-P (1982) A thermochemical study of glasses and crystals along the joins silica-calcium aluminate and silica-sodium aluminate. Geochim Cosmochim Acta 46:2039–2047. https://doi.org/10.1016/0016-7037(82)90183-1

Neuville DR, Cormier L, Flank A-M, Briois V, CASsiot D (2004) Al speciation and Ca environment in calcium aluminosilicate glasses and crystals by Al and Ca K-edge X-ray absorption spectroscopy. Chem Geol 213:153–163. https://doi.org/10.1016/j.chemgeo.2004.08.039

Okuno M, Marumo F (1993) The structure analyses of pyrope ($Mg_3Al_2Si_3O_{12}$) and grossular ($Ca_3Al_2Si_3O_{12}$) glasses by X-ray diffraction method. Mineral J 16:407–415. https://doi.org/10.2465/minerj.16.407

Polian A, Grimsditch M (1993) Sound velocities and refractive index of densified *a*-SiO_2 to 25 GPa. Phys Rev B 47:13979–13982. https://doi.org/10.1103/PhysRevB.47.13979

Price DL, Moss SC, Reijers R, Saboungi M-L, Susman S (1988) Intermediate-range order in glasses and liquids. J Phys C Solid State Phys 21:L1069–L1072. https://doi.org/10.1088/0953-8984/1/5/017

Renou R, Soulard L, Lescoute E, Dereure C, Loison D, Guin J-P (2017) Silica glass structural properties under elastic shock compression: experiments and molecular simulations. J Phys Chem C 121:13324–13334. https://doi.org/10.1021/acs.jpcc.7b01324

Russell JK, Giordano D (2005) A model for silicate melt viscosity in the system $CaMgSi_2O_6$–$CaAl_2Si_2O_8$–$NaAlSi_3O_8$. Geochim Cosmochim Acta 69:5333–5349. https://doi.org/10.1016/j.gca.2005.06.019

Sakamaki T, Kono Y, Wang Y, Park C, Yu T, Jing Z, Shen G (2014) Contrasting sound velocity and intermediate-range structural order between polymerized and depolymerized silicate glasses under pressure. Earth Planet Sci Lett 391:288–295. https://doi.org/10.1016/j.epsl.2014.02.008

Sanchez-Valle C, Bass JD (2010) Elasticity and pressure-induced structural changes in vitreous $MgSiO_3$-enstatite to lower mantle pressures. Earth Planet Sci Lett. https://doi.org/10.1016/j.epsl.2010.04.034

Sato T, Funamori N (2010) High-pressure structural transformation of SiO_2 glass up to 100 GPa. Phys Rev B. https://doi.org/10.1103/PhysRevB.82.184102

Schroeder J, Bilodeau TG, Zhao X-S (1990) Brillouin and Raman scattering from glasses under high pressure. High Press Res 4:531–533. https://doi.org/10.1080/08957959008246178

Shannon RD (1976) Revised effective ionic radii and systematic studies of interatomic distances in halides and chalcogenides. Acta Crystallogr A 32:751–767. https://doi.org/10.1107/S0567739476001551

Shimoda K, Miyamoto H, Kikuchi M, Kusaba K, Okuno M (2005) Structural evolutions of $CaSiO_3$ and $CaMgSi_2O_6$ metasilicate glasses by static compression. Chem Geol 222:83–93. https://doi.org/10.1016/j.chemgeo.2005.07.003

Shimoda K, Tobu Y, Hatakeyama M, Nemoto T, Saito K (2007) Structural investigation of Mg local environments in silicate glasses by ultra-high field ^{25}Mg 3QMAS NMR spectroscopy. Am Mineral 92:695–698. https://doi.org/10.2138/am.2007.2535

Stebbins JF, Xu Z (1997) NMR evidence for excess non-bridging oxygen in an aluminosilicate glass. Nature 390:60–62. https://doi.org/10.1038/36312

Stebbins JF, Wu J, Thompson LM (2013) Interactions between network cation coordination and non-bridging oxygen abundance in oxide glasses and melts: insights from NMR spectroscopy. Chem Geol 346:34–46. https://doi.org/10.1016/j.chemgeo.2012.09.021

Suito K, Miyoshi M, Sasakura T, Fujisawa H (1992) Elastic properties of obsidian vitreous SiO_2 and vitreous GeO_2 under high pressure up to 6 GPa. In: Syono Y, Manghnani MH (eds) High pressure research: applications to earth and planetary sciences. Terra Scientific Publishing Company, Tokyo, pp 209–211

Sun N, Stixrude L, de Koker N, Karki BB (2011) First principles molecular dynamics simulations of diopside ($CaMgSi_2O_6$) liquid to high pressure. Geochim Cosmochim Acta 75:3792–3802. https://doi.org/10.1016/j.gca.2011.04.004

Susman S, Volin KJ, Montague DG, Price DL (1990) The structure of vitreous and liquid $GeSe_2$: a neutron diffraction study. J Non-Cryst Solids 125:168180. https://doi.org/10.1016/0022-3093(90)90336-K

Taylor M, Brown GE (1979) Structure of mineral glasses—II. The SiO_2–$NaAlSiO_4$ join. Geochim Cosmochim Acta 43:1467–1473. https://doi.org/10.1016/0016-7037(79)90141-8

Uchino T, Sakka T, Ogata Y, Iwasaki M (1993) Local structure of sodium aluminosilicate glass: an ab initio molecular orbital study. J Phys Chem 97:9642–9649. https://doi.org/10.1021/j100140a019

Walker AM, Sullivan LA, Trachenko K, Bruin RP, White TOH, Dove MT, Tyer RP, Todorov IT, Wells SA (2007) The origin of the compressibility anomaly in amorphous silica: a molecular

dynamics study. J Phys: Condens Matter 19:275210. https://doi.org/10.1088/0953-8984/19/27/275210

Weigel C, Le Losq C, Vialla R, Dupas C, Clément S, Neuville DR, Ruffl é B (2016) Elastic moduli of $XAlSiO_4$ aluminosilicate glasses: effects of charge-balancing cations. J Non-Cryst Solids 447:267–272. https://doi.org/10.1016/j.jnoncrysol.2016.06.023

Whittington A, Richet P, Holtz F (2000) Water and the viscosity of depolymerized aluminosilicate melts. Geochim Cosmochim Acta 64:3725–3736. https://doi.org/10.1016/S0016-7037(00)00448-8

Xiang Y, Du J, Smedskjaer MM, Mauro JC (2013) Structure and properties of sodium aluminosilicate glasses from molecular dynamics simulations. J Chem Phys 139:044507. https://doi.org/10.1063/1.4816378

Yokoyama A, Matsui M, Higo Y, Kono Y, Irifune T, Funakoshi K (2010) Elastic wave velocities of silica glass at high temperatures and high pressures. J Appl Phys 107:123530. https://doi.org/10.1063/1.3452382

Yue Y, Christiansen J (1999) Fragility and flow behaviour of several phosphate and silicate melts. Phosphorus Res Bull 10:497–502. https://doi.org/10.3363/prb1992.10.0_497

Zha C, Hemley RJ, Mao H, Duffy TS, Meade C (1994) Acoustic velocities and refractive index of SiO_2 glass to 57.5 GPa by Brillouin scattering. Phys Rev B 50:13105–13112. https://doi.org/10.1103/PhysRevB.50.13105